Structural Engineering and Mechanics, *Vol. 73, No. 2 (2020) 143-152*
DOI: https://doi.org/10.12989/sem.2020.73.2.143

Shear mechanism of steel fiber reinforced concrete deep coupling beams

Kou Li[1a], Jun Zhao[*1] and Wenbo Ren[2b]

[1]*School of Mechanics and Engineering Science, Zhengzhou University, 100 Science Avenue, Zhengzhou 450001, China*
[2]*School of Civil Engineering, Zhengzhou University, 100 Science Avenue, Zhengzhou 450001, China*

(Received November 12, 2018, Revised July 18, 2019, Accepted August 27, 2019)

Abstract. Deep coupling beams are more prone to suffer brittle shear failure. The addition of steel fibers to seismic members such as coupling beams can improve their shear performance and ductility. Based on the test results of steel fiber reinforced concrete(SFRC) coupling beams with span-to-depth ratio between 1.5 and 2.5 under lateral reverse cyclic load, the shear mechanism were analyzed by using strut-and-tie model theory, and the effects of the span-to-depth ratio, compressive strength and volume fraction of steel fiber on shear strengths were also discussed. A simplified calculation method to predict the shear capacity of SFRC deep coupling beams was proposed. The results show that the shear force is mainly transmitted by a strut-and-tie mechanism composed of three types of inclined concrete struts, vertical reinforcement ties and nodes. The influence of span-to-depth ratio on shear capacity is mainly due to the change of inclination angle of main inclined struts. The increasing of concrete compressive strength or volume fraction of steel fiber can improve the shear capacity of SFRC deep coupling beams mainly by enhancing the bearing capacity of compressive struts or tensile strength of the vertical tie. The proposed calculation method is verified using experimental data, and comparative results show that the prediction values agree well with the test ones.

Keywords: steel fiber concrete; deep coupling beams; strut-and-tie model; shear mechanism; shear capacity

1. Introduction

Coupling beams with small span-to-depth ratio are widely used in the shear wall structures due to the structural design requirements. In order to improve the seismic behavior of the coupling beam, a large number of steel bars are used in deep coupling beams because of the low tensile strength of conventional concrete, which causes the severe reinforcement congestion problem. Therefore, some studies focus on material properties to improve the seismic behavior of coupling beams. Parra-Montesinos (2005) discussed the potential of high-performance fiber-reinforced cement composites (HPFRCCs) for the use in earthquake-resistant structures, and indicated that the use of HPFRCC materials could increase displacement capacity of flexural and shear-critical members and exhibited outstanding damage tolerance. Canbolat et al. (2005) and Lequesne (2013) conducted the experimental research of the coupling beams using high-performance fiber-reinforced cement composites. The results showed that HPFRCCs could effectively improve the seismic behavior and shear capacity of coupling beams. A research project was carried out by Chaallal *et al*. (1996) to examine the performance of steel fiber reinforced concrete (SFRC) wall/coupling beam joint under cyclic loading. The results showed that SFRC wall/coupling beam joint exhibited higher ultimate capacities at similar ductility than conventional concrete, and it was viable to apply SFRC to seismic regions to enhance structural integrity and ease steel congestion problem.

Zhang *et al*. (2007) has completed experimental program of 13 steel fiber reinforced concrete deep coupling beams with span-to-depth ratio no more than 2.5, it was observed that the energy dissipation capacities of steel fiber reinforced concrete coupling beams were better than conventional reinforced concrete coupling beams, and replacing part of stirrups with moderate amount of steel fibers could effectively reduce the capacity degradation speed of coupling beams. Several works studied the seismic behavior of steel fiber reinforced concrete coupling beams under lateral reverse cyclic loading (Li 2012, Jia 2012, Ma 2011), the main test parameters were span-to-depth ratio, volume fraction of steel fiber and concrete strength. The results demonstrated that the use of steel fiber could effectively improve the bearing capacity, ductility and energy dissipation capacity of deep coupling beams with conventional reinforcement, and the failure mode gradually changed from shear failure to flexure-shear failure with the increase of volume fraction of steel fiber. An experimental program on the monotonic tests was performed to analyze the shear performance of steel fiber reinforced concrete coupling beams with span-to-depth ratio of 1.0, 1.5, 2.0 (Kuang and Baczkowski 2006, 2009). The results illustrated that the steel fiber reinforced concrete coupling beams had a higher shear capacity than conventional reinforced concrete coupling beams.

*Corresponding author, Professor
E-mail: zhaoj@zzu.edu.cn
[a] Ph.D. Student
E-mail: zzucocolee@foxmail.com
[b] Ph.D. Student
E-mail: tomhi@qq.com

http://www.techno-press.com/journals/sem&subpage=7 ISSN: 1225-4568 (Print), 1598-6217 (Online)

Table 1 Summary of the specimens (Cai *et al*. 2016)

Beam number	b (mm)	h (mm)	l_n/h	f_{fcu} (MPa)	f_{fct} (MPa)	Steel fiber V_{sf}	Steel fiber Type	Steel fiber α_f	Steel Stirrup f_{yv} (MPa)	Steel Stirrup ρ_v (%)	Steel Longitudinal bar f_y (MPa)	Steel Longitudinal bar ρ (%)
CCB3-40-2.5-1F-F/S	150	400	2.5	43.1	3.26	1.0%						
CCB3-30-2-1F-S	150	400	2.0	40.5	2.62	1.0%						
CCB3-40-2-1F-S	150	400	2.0	43.1	3.26	1.0%						
CCB3-50-2-1F-S	150	400	2.0	52.9	3.63	1.0%						
CCB3-60-2-1F-S	150	400	2.0	66.7	4.27	1.0%						
CCB3-70-2-1F-S	150	400	2.0	70.1	4.54	1.0%						
CCB3-80-2-1F-S	150	400	2.0	80.7	5.44	1.0%	Crimped	42	295.6	0.056	363.4	1.17
CCB3-50-2-0F-S	150	400	2.0	55.6	3.40	0%						
CCB3-50-2-0.5F-S	150	400	2.0	54.5	3.82	0.5%						
CCB3-50-2-1F-S	150	400	2.0	54.8	4.64	1.0%						
CCB3-50-2-1.5F-S	150	400	2.0	55.9	5.51	1.5%						
CCB3-50-2-2F-S	150	400	2.0	55.3	5.96	2.0%						
CCB3-50-2-2.5F-F/S	150	400	2.0	54.1	6.66	2.5%						

Where b and h are section width and height of coupling beams, respectively; l_n/h is span-to-depth ratio; f_{fcu} and f_{fct} are compressive strength and tensile strength of steel fiber concrete, respectively; V_{sf} is volume fraction of steel fiber; α_f is length to diameter ratio of steel fiber; f_{yv} and ρ_v are yielding strength and reinforcement ratio of stirrup, respectively; f_y and ρ are tensile strength and reinforcement ratio of longitudinal bar, respectively.

On the basis of experimental researches, theoretical analyses of coupling beams are also intensively investigated (Bhunia et al. 2007, Lee et al. 2008, Mihaylov and Franssen 2017). Coupling beams with span-to-depth ratio no more than 2.5 belong to the deep member which do not obey the plane-section hypothesis. Strut-and-tie model is considered to be an effective method to analyze the complicated stress state of such regions. It has been adopted in concrete structure design standard of many countries, such as United States (ACI 318-14, 2014), Canada (CSA Committee A23.3, 2004), New Zealand (NZS 3101, 2006) and so on. Deng *et al*. (2018) proposed the modified direct strut-and-tie model to determine the shear strength of highly ductile fiber reinforced concrete deep beams, and the model showed good agreement with the test results. Yavuz (2016) studied the accuracy of the strut-and-tie model in ACI318-14 in predicting the shear strength of reinforced concrete deep beams. The results show that the strut-and-tie model method in ACI318-14 is conservative. Hanoon *et al*. (2017) used strut-and-tie model to estimate the shear capacity of reinforced concrete deep beams strengthened with carbon fiber-reinforced polymer sheets. Strut-and-tie model design method is developed based on the actual stress state of the component, and the complex stress state is simplified as a truss system consisting of a series of struts and ties. The concrete struts are set in the main compression zone, and tension ties are represented by the reinforcements to transmit tensile stress. The key point to establish an available strut-and-tie model is to understand the force transfer mechanism within the components (Schlaich *et al*. 1987).

The shear force is resisted primarily by one inclined strut from the loading point to the support point in deep beams. According to ACI 318-14 Code, the effective inclination angle of strut is range from 26.6° to 63.5° and a conservation estimate of the strength in beams was considered by Matamoros and Wong (2003) with strut inclination angles ranging between 30 and 60 degrees (shear span -to-depth ratio ranging between approximately 0.5 and 1.5). For deep coupling beams with span-to-depth ratio more than 1.5, the diagonal compression forces cannot be transferred directly between two compressive end zone because the inclination angle of the struts along the shear span is too small. This paper focuses on the shear mechanism analysis of steel fiber reinforced coupling concrete beams with span-to-depth ratio between 1.5 and 2.5 using strut-and-tie model. Then, the effects of three test parameters on shear capacity of SFRC coupling beams with span-to-depth ratio between 1.5 and 2.5 are investigated. Finally, a simplified prediction method based on the strut-and-tie model is proposed for shear capacity of SFRC coupling beams with span-to-depth ratio between 1.5 and 2.5.

2. Experimental investigation

A total of thirteen SFRC coupling beams with span-to-depth ratio between 1.5 and 2.5 have been manufactured and tested (Cai *et al*. 2016). Test parameters included the span-to-depth ratio, compressive strength of steel fiber concrete and volume fraction of steel fiber. The details of these SFRC specimens and the properties of materials are shown in Table 1 and Fig. 1. The last four items of the beam numbers shown in Table 1 indicate the concrete strength grade, span-to-depth ratio, volume fraction of steel fiber,

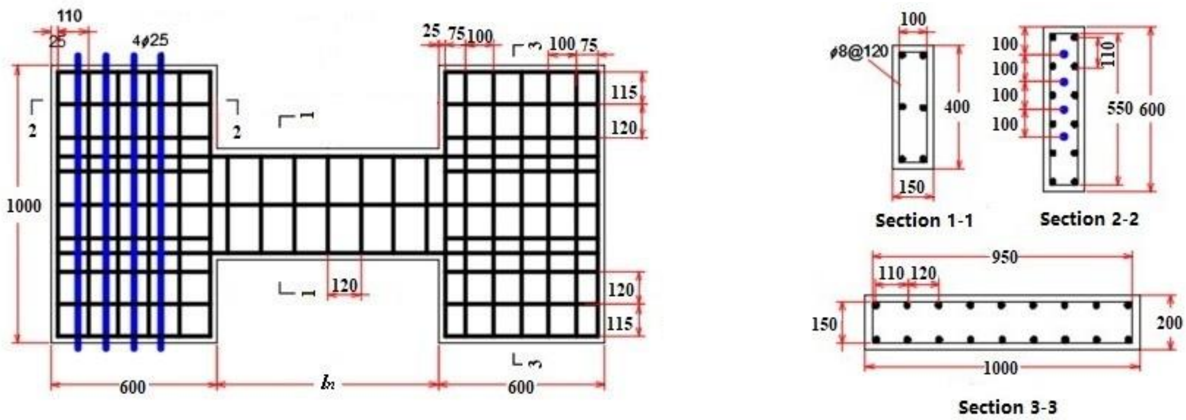

Fig. 1 Dimensions and reinforcement details of specimens (Cai *et al*. 2016)

and failure mode of specimens, respectively, where S means the shear failure mode and F/S means flexure-shear failure mode.

3. Shear mechanism analysis

3.1 Cracking pattern

The cracking characteristics of SFRC coupling beams with span-to-depth ratio between 1.5 and 2.5 are discussed according to the test results obtained from Cai *et al*. (2016), in order to analyze the shear mechanism of SFRC deep coupling beams. Fig. 2 shows the cracking patterns of SFRC coupling beams with span-to-depth ratio between 1.5 and 2.5. It could be observed that the main diagonal cracks of these coupling beams developed from beam ends to mid-span, and two "X"-type main cracks were finally formed due to the lateral reverse cyclic loading. In addition, several inclined cracks formed in the triangular region between the beam end and the main cracks, and these cracks dispersed along the fan-shaped direction were called fan-shaped inclined cracks. Some subtle inclined cracks which parallel to the main diagonal cracks were observed in most of specimens, and the concrete around these cracks was relatively integrity when the specimens reach their ultimate capacity. It can be observed that the number of inclined cracks increases with the increase of volume fraction of steel fiber, while the crack widths decrease, which indicate that the addition of steel fiber can enhance the aggregate interlock of concrete and control cracks development.

3.2 Shear transfer mechanism based on strut-and-tie model

According the above discussed cracking characteristics, a strut-and-tie model can be established to simulate the shear transfer mechanism of coupling beams with span-to-depth ratio between 1.5 and 2.5, as shown in Fig. 3. The compressive zones are modeled as concrete struts including three type, namely main inclined struts, fan-shaped secondary struts and parallel secondary struts. These concrete struts are located between cracks based on the test results. The ties used here are based on the location of the reinforcements in the coupling beams specimens. The contribution of discontinuous steel fibers should be considered as reinforcement ties to bridge cracks and transmit tensile stress, then resisting shear force together with vertical stirrups. In addition, due to the small widths of the parallel cracks observed in the experiment, the corresponding parallel secondary struts can be negligible when the strut-and-tie model is used in calculation. The failure mode can be expected include crushing of struts and yielding of tie, which are referred to as shear-compression failure mode and shear-tension failure mode.

4. Effects of test parameters on shear strength

The previous experimental results conducted by Cai *et al*. (2016), Kuang *et al*. (2009), Kwan *et al*. (2002) showed that span-to-depth ratio, compressive strength of fiber concrete and volume fraction of steel fiber could influence the shear strength of SFRC coupling beams with span-to-depth ratio between 1.5 and 2.5. According to the above shear transfer strut-and-tie model, how the three test parameters influence the shear capacity of SFRC deep coupling beams is discussed in the following.

4.1 Effect of span-to-depth ratio

The effect of span-to-depth ratio on shear strength taken from the experimental results conducted by Cai *et al*. (2016), Kuang *et al*. (2009), Kwan *et al*. (2002) is shown in Table 2. The results show that the shear capacity of deep coupling beam with a low span-to-depth ratio is higher than that with a higher span-to-depth ratio. It can be explained based on the above shear transfer strut-and-tie model. The influence of span-to-depth ratio on shear capacity is mainly due to the change of inclination angle of main inclined struts. The vertical component of force in the main inclined strut can resist the shear force at the end of coupling beam. The increase of span-to-depth ratio decreases the angle between the main inclined strut and the longitudinal axis of the coupling beams, thus increases the compressive stress generated in the main inclined strut when the same shear

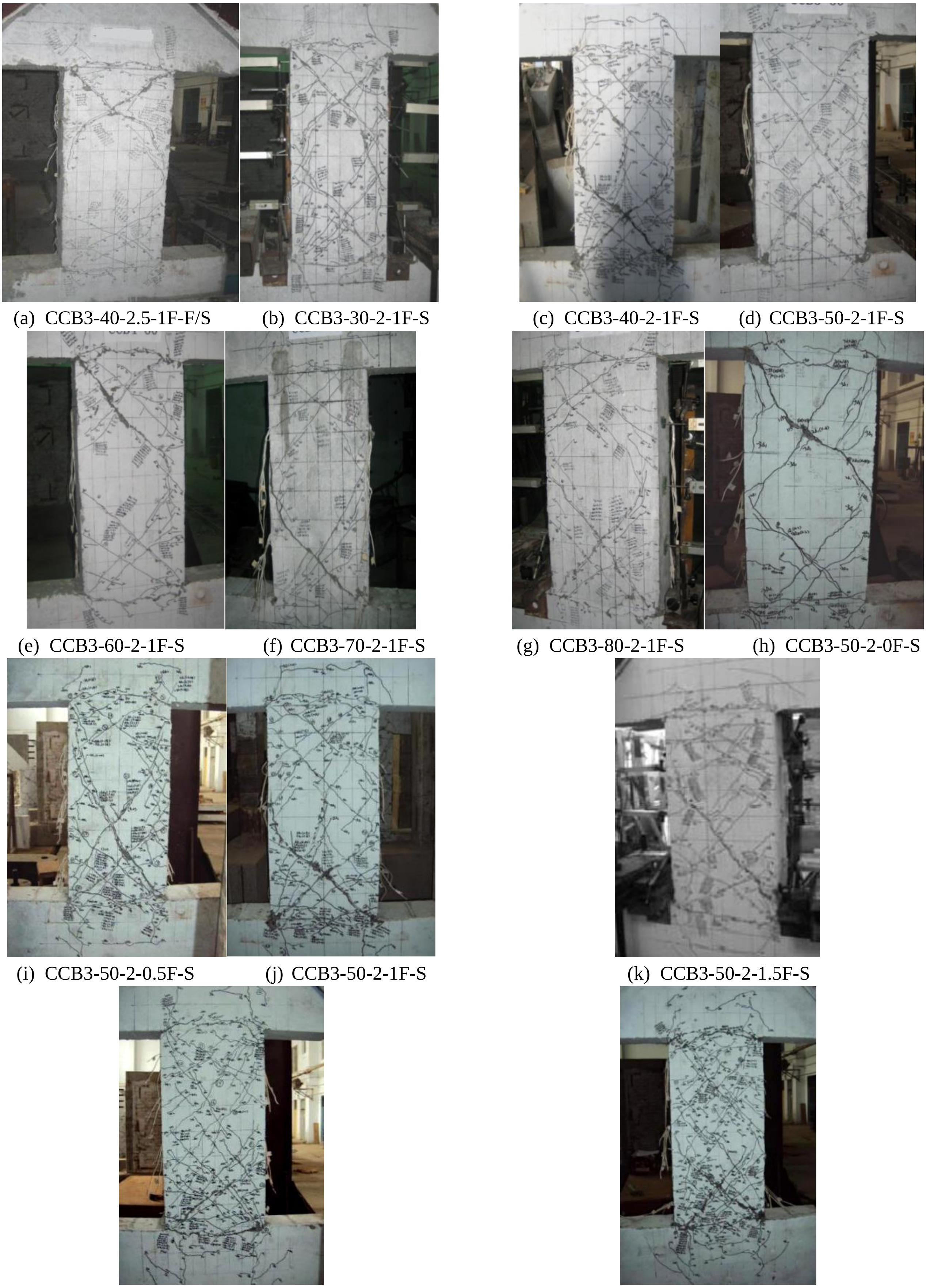

(a) CCB3-40-2.5-1F-F/S (b) CCB3-30-2-1F-S (c) CCB3-40-2-1F-S (d) CCB3-50-2-1F-S

(e) CCB3-60-2-1F-S (f) CCB3-70-2-1F-S (g) CCB3-80-2-1F-S (h) CCB3-50-2-0F-S

(i) CCB3-50-2-0.5F-S (j) CCB3-50-2-1F-S (k) CCB3-50-2-1.5F-S

(l) CCB3-50-2-2F-S (m) CCB3-50-2-2.5F-F/S

Fig. 2 Cracking patterns of SFRC coupling beams with span-to-depth ratio between 1.5 and 2.5 (Cai *et al*. 2016)

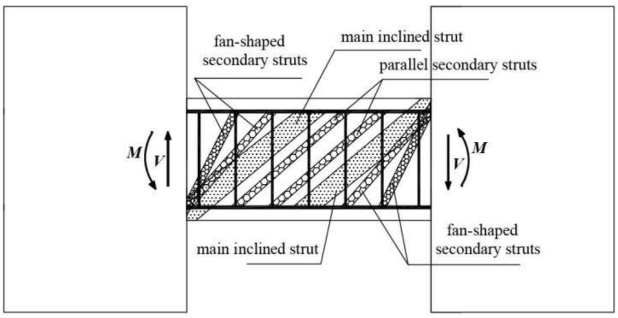

Fig. 3 Shear mechanism model of SFRC coupling beams with span-to-depth ratio between 1.5 and 2.5

Table 2 Effect of span-to-depth ratio on the measured shear capacity of specimens

Reference	l_n/h	b (mm)	h (mm)	V_{sf} (%)	f_{fc}' (MPa)	V_t (kN)	V_t $/(bdf_{fc}')$
Cai *et al.* (2016)	2.00	150	400	1.0	34.10	238	0.13
	2.50	150	400	1.0	34.10	190	0.11
Kuang *et al.* (2009)	1.67	100	400	1.0	38.16	281.5	0.21
	2.22	100	400	1.0	38.72	262.2	0.19
Kwan *et al.* (2002)	1.75	120	400	0	37.80	165	0.10
	2.00	120	350	0	37.80	123	0.09

force at the beam-end is transmitted. Therefore, the shear capacity of coupling beam decreases with increasing span-to-depth ratio because the main inclined strut in the coupling beam with larger span-to-depth ratio is more likely to be crushed.

4.2 Effect of fiber concrete compressive strength

The effect of the fiber concrete compressive strength on shear strength taken from the experimental results conducted by Cai *et al.* (2016) is shown in Fig. 4. These SFRC specimens have the same span-to-depth ratio of 2.0 and steel fiber volume fraction of 1.0%. The vertical axis in the Fig. 4 represents the measured shear strength V_t, while the horizontal axis represents the fiber concrete compressive strength f_{fcu}. It can be noted that the shear capacities of SFRC coupling beams increase with increasing fiber concrete compressive strength.

The shear force at the beam end was transmitted through the above strut-and-tie model. If the steel fiber concrete strut reached ultimate state earlier than the vertical tie formed by stirrups and steel fibers, such as 40.5 MPa used in this study, the shear-compression mode would occur. The SFRC coupling beams would fail due to the crushed inclined concrete strut, and their shear capacity mainly depended on the compressive strength of the steel fiber concrete strut. The bearing capacity of concrete strut increased with the increase of concrete compressive strength. If the vertical tie reached its ultimate state firstly, the specimen would fail as a shear-tension mode, such as the specimen from CCB3-40-2-1F-S to CCB3-80-2-1F-S, and their shear capacity mainly depended on the tensile strength of vertical tie which was contributed by stirrups

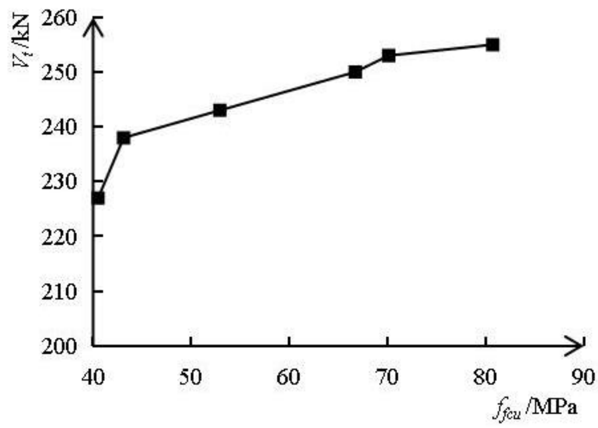

Fig. 4 Effect of concrete compressive strength on the measured shear capacity of specimens

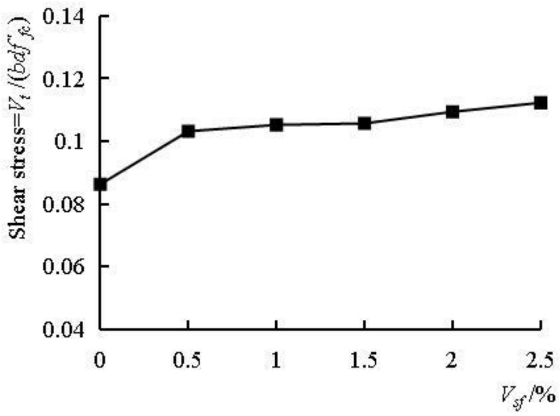

Fig. 5 Effect of volume fraction of steel fiber on the measured shear capacity of specimens

and steel fibers. The specimens in Fig. 4 only had differences in compressive strength of concrete. However, the compressive strength of concrete could affect the initial bonding stress between steel fibers and concrete matrix. The initial bonding stress of steel fibers increased with increasing concrete strength (Naaman 1991), which means that the high strength concrete can improve the tensile resistance of steel fibers. Therefore, regarding the specimen from CCB3-40-2-1F-S to CCB3-80-2-1F-S which failed as a shear-tension mode, the increase in the shear capacity with increasing concrete compressive strength is attributed to the fact that the tensile strength of vertical tie is enhanced due to the increased tensile resistance of steel fibers.

4.3 Effect of volume fraction of steel fiber

The variations in ultimate shear capacity with the steel fiber volume fraction are shown in Fig. 5 (Cai *et al.* 2016). These SFRC specimens have the same span-to-depth ratio of 2.0 and fiber reinforced concrete strength grade of CF50. Fig. 5 shows that the shear stresses ($V_t/(bdf_{fc}')$) increase effectively when the volume fractions of steel fiber increase from 0% to 0.5%, which indicates that the addition of steel fiber have a significant influence on shear capacity of deep coupling beams. As the volume fraction of steel fibers

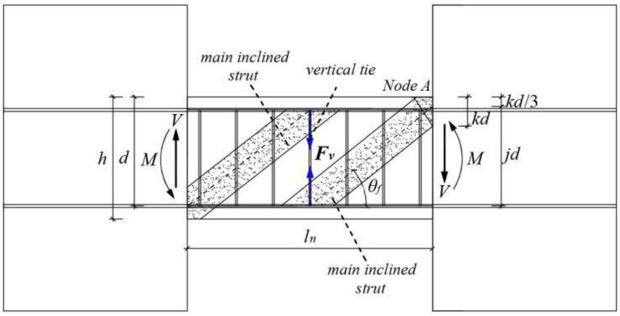

Fig. 6 Calculating diagram based on strut-and-tie model of coupling beams

continues to increase, the failure modes were changed from shear-tension failure to shear-compression failure. This indicated that the increase of fiber volume fraction could enhance the tensile strength of the vertical tie, which made the bearing capacity of vertical tie greater than that of concrete strut in the shear transfer strut-and-tie model. Therefore, the SFRC coupling beams failed as a shear-compression mode, and the shear capacity depended on the compressive strength of the concrete strut. These SFRC coupling beams had little difference in measured fiber concrete compressive strength, so the shear capacity didn't change obviously. When the steel fiber volume fraction reached 2.5%, a large amount of distributed steel fiber could transfer stresses across the matrix and prohibited the propagation of crack once the matrix cracked. The failure modes of SFRC coupling beams were changed from shear failure to flexure-shear failure, which was also benefit to the shear capacity of SFRC coupling beams.

5. Proposed method

On the basis of the above shear transfer strut-and-tie model, a shear prediction method is proposed in this section. Fig. 6 shows the simplified strut-and-tie model for shear calculation which consists of main inclined struts composed of steel fiber concrete and vertical tie composed of stirrups and steel fibers. When the coupling beam reaches its ultimate state, it is considered that the shear capacity is related to the bearing capacity of the inclined strut and vertical tie.

5.1 Main inclined struts

θ_f is the inclination angle of the main inclined struts to the longitudinal axis of the coupling beam and can be determined by Eq. (1) as follows (Hwang *et al*. 2000).

$$\tan\theta_f = \frac{jd}{0.5l_n} = \frac{2d(1-k/3)}{l_n} \tag{1}$$

Where, l_n is the length of coupling beam; d is effective height of the coupling beam; jd is the distance of the lever arm from the resultant compressive force to the centroid of the longitudinal tension reinforcement; kd is depth of compression zone at cross section; according to reference (Thomas and Mo 2010), the coefficient k can be expressed as Eq. (2).

$$\begin{aligned} k = & \sqrt{\left[n\rho+(n-1)\rho'\right]^2 + 2\left[n\rho+(n-1)\rho' d'/d\right]} \\ & -\left[n\rho+(n-1)\rho'\right] \end{aligned} \tag{2}$$

Where $n=E_s/E_c$, E_s and E_c are the elastic modulus ratio of longitudinal reinforcement and concrete, respectively; ρ is the ratio of tension reinforcement; ρ' is the ratio of compression reinforcement; d' is the distance from centroid of the compression reinforcement to compression zone's edge.

The effective area of main inclined strut A_{str} can be estimated as

$$A_{str} = a_s \times b_s = kdb/\cos\theta_f \tag{3}$$

Where a_s is depth of the main inclined strut; b_s is the width of the main inclined strut and can be defined as width of coupling beam b.

The effective compressive strength of strut f_{ce} can be calculated by Eq. (4), where ζ is the softening coefficient of concrete and can be calculated by Eq. (5) according to reference (Hwang and Lee 2002, Pauletta *et al*. 2015), where f'_{fc} is cylinder compressive strength of fiber concrete.

$$f_{ce} = \zeta f'_{fc} \tag{4}$$

$$\zeta \approx \frac{3.35}{\sqrt{f'_{fc}}} \leq 0.52 \tag{5}$$

The bearing capacity of main inclined strut can be calculated by Eq. (6) as follows.

$$F_c = A_{str} f_{ce} = kdb\zeta\, f'_{fc}/\cos\theta_f \tag{6}$$

5.2 Vertical tie

Ignoring the tensile strength of concrete, the bearing capacity of vertical tie F_v is contributed by stirrups and steel fibers. The bearing capacity of stirrups vertical tie F_{sv} can be calculated by Eq. (8).

$$F_v = F_{sv} + F_{sf} \tag{7}$$

$$F_{sv} = A_{sv} f_{yv} = \eta_1 n_{sv} A_{sv1} f_{yv} \tag{8}$$

Where f_{yv} is yielding stress of stirrups, A_{sv} is cross sectional area of stirrups vertical tie, η_1 is the coefficient of shear resistance; n_{sv} is the number of stirrups; A_{sv1} is the cross section area of single stirrup. According to reference (Kuo *et al*. 2010), the coefficient of shear resistance η_1 equals to 0.75 when estimate the effectiveness of the vertical tie.

The randomly distributed steel fibers that across the cracks can be equivalent to vertical tie to transfer shear stress. The bearing capacity of steel fibers vertical tie F_{sf}

can be calculated by Eq. (9).

$$F_{sf} = A_{sf,v} f_{sf} \tag{9}$$

Where f_{sf} is average shear stress of steel fibers. The equivalent cross section area of the steel fibers vertical tie $A_{sf,v}$ can be estimated by Eq. (10) (Gao *et al*. 2014).

$$A_{sf,v} = \eta_1 \eta_2 V_{sf} \frac{bl_j}{\cos\theta_c} \tag{10}$$

The direction coefficient of steel fibers η_2 can be approximated as 0.41 (Romualdi and Mandel 1964); l_j is the projected length of the main crack in the horizontal direction; V_{sf} is volume fraction of steel fiber; θ_c is the angle between the main crack and the horizontal direction, and can be considered as the inclination angle of main inclined strut θ_f.

The steel fibers across the cracks become effectively engaged in the shear transfer mechanism due to the bond between the fiber and cementitious matrix after the cracks appear. According to reference (Gao *et al*. 2014), f_{sf} is considered as Eq. (11).

$$f_{sf} = D_{sf} \alpha_f \tau_{sf,\max} \le f_{yf} \tag{11}$$

Where f_{yf} is the ultimate tensile strength of steel fiber; D_{sf} is type impact coefficient of steel fiber, which is taken as 0.5, 0.75 and 1.0 for straight, crimped and end hooked steel fiber, respectively; α_f is length to diameter ratio of steel fiber; $\tau_{sf,\max}$ is maximum bond shear stress between steel fiber and concrete, according to reference (Ng *et al*. 2012), $\tau_{sf,\max}$ and mean tensile strength of concrete matrix f_{ct} have following relationship approximately. The coefficient k_b is taken as 0.4, 0.8 and 1.0 for straight, end hooked and crimped steel fibers, respectively.

$$\tau_{sf,\max} = 3k_b f_{ct} \tag{12}$$

5.3 Solution procedure

The equilibrium condition between the shear force V, the bearing capacity of main inclined strut F_c and the bearing capacity of vertical tie F_v are expressed by Eqs. (13) -(14).

$$V = F_c \sin\theta_f \tag{13}$$

$$V = F_v \tag{14}$$

The major failure mode of deep beams is the crushing of compression strut (Hwang *et al*. 2000). The shear calculation processes are concluded as follows. First, it can be assumed that the coupling beam reaches its ultimate bearing capacity due to the crushing of the main inclined strut, and the bearing capacity of main inclined strut F_c can be determined according to Eq. (6). Next, the shear force V at the beam-end and the bearing capacity of vertical tie F_v can be determined according to Eqs. (13)-(14). Finally, the calculated F_v is compared with the bearing capacity of the vertical tie determined by Eq. (7) to verify whether the vertical tie reaches its limit state. If the vertical tie doesn't reach its limit state, the shear force that causes the failure of main inclined strut is taken as the shear capacity of the coupling beam; if the vertical tie has reached its limit state, the shear capacity is determined by Eq. (7) and Eq. (14).

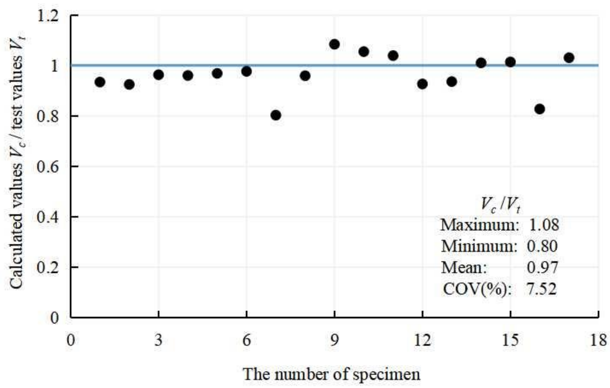

Fig. 7 Comparison between calculated and test results

6. Comparison of experimental results and predictions

The proposed model was verified using experimental data of steel fiber reinforced concrete coupling beams with span-to-depth ratio $1.5<l_n/h\le 2.5$ in reference Zhang *et al*. (2007) and Cai *et al*. (2016). The comparison between the calculated values V_c and the test results V_t are given in Table 3 and Fig. 7. The average ratio of V_c/V_t is 0.97 with a coefficient of variation of 7.52%. The results show that the predictions are in good agreement with the experimental results.

7. Conclusions

This paper discussed the shear transfer mechanism of SFRC coupling beams with span-to-depth ratio between 1.5 and 2.5 based on the strut-and-tie model, and three test variables including span-to-depth ratio, fiber concrete compressive strength and volume fraction of steel fiber were also investigated from the aspect of the proposed shear transfer strut-and-tie model. Then, the shear strengths of the tested SFRC coupling beams were predicted using the strut-and-tie model. The main results of the study can be summarized as follows:

- The shear transfer mechanism of the SFRC coupling beam with span-to-depth ratio between 1.5 and 2.5 can be simulated as a strut-and-tie model, which composed of three types of inclined concrete struts, vertical reinforcement ties consisting of steel fibers and stirrups and nodes.
- The influence of span-to-depth ratio on shear capacity is mainly due to the change of inclination angle of

Table 3 Comparison between predictions and test results

Reference	Specimen number	l_n/h	f_{fcu} (MPa)	Stirrup	f_{yv} (MPa)	Steel fiber V_{sf}	Steel fiber α_f	Steel fiber Type	V_c (kN)	V_t (kN)	V_c/V_t
Zhang *et al.* (2007)	CCB1-3	1.75	75.3	ϕ8@150	350.0	0.75%	75	End hooked	204	218	0.94
	CCB1-4	2.0	73.6			0.75%			197	195	1.01
	CCB1-5	2.5	78.3			0.75%			148	146	1.01
	CCB2-3	1.75	69.8			0.5%			172	208	0.83
	CCB2-4	1.75	66.3			1.0%			236	229	1.03
Cai *et al.* (2016)	CCB3-40-2.5-1F-F/S	2.5	43.1	ϕ8@150	295.6	1.0%	42	Crimped	176	190	0.93
	CCB3-30-2-1F-S	2.0	40.5			1.0%			212	227	0.93
	CCB3-40-2-1F-S	2.0	43.1			1.0%			220	238	0.93
	CCB3-50-2-1F-S	2.0	52.9			1.0%			234	243	0.96
	CCB3-60-2-1F-S	2.0	66.7			1.0%			240	250	0.96
	CCB3-70-2-1F-S	2.0	70.1			1.0%			245	253	0.97
	CCB3-80-2-1F-S	2.0	80.7			1.0%			249	255	0.98
	CCB3-50-2-0.5F-S	2.0	54.5			0.5%			191	238	0.80
	CCB3-50-2-1F-S	2.0	54.8			1.0%			234	244	0.96
	CCB3-50-2-1.5F-S	2.0	55.9			1.5%			271	250	1.08
	CCB3-50-2-2F-S	2.0	55.3			2.0%			270	256	1.05
	CCB3-50-2-2.5F-F/S	2.0	54.1			2.5%			267	257	1.04

main inclined struts. The increasing of concrete compressive strength can improve the shear capacity of SFRC deep coupling beams by enhancing the bearing capacity of compressive struts, and the addition of steel fiber has an effective influence on shear capacity because the increase of fiber volume fraction could enhance the tensile strength of the vertical tie.

- The proposed calculation method based on strut-and-tie model show good shear prediction capability of SFRC coupling beams with span-to-depth ratio between 1.5 and 2.5 compared with the test results.

Acknowledgments

This work was supported by the National Key R&D Program of China [grant number 2016YFE0125600], National Natural Science Foundation of China [grant number 51078333]; Program for Changjiang Scholars and Innovative Research Team in University of Minister of Education of China [grant number IRT_16R67]. These supports are gratefully acknowledged. In addition, the authors specially thank to Mr. Xin Ma, Bo Jia and Bin Li for their helps in the tests.

References

ACI 318 (2014), Building code requirements for structural concrete and commentary, American Concrete Institute; Farmington Hills, MI, USA.

Bhunia, D., Parkash, V. and Pandey, A.D. (2007), "A procedure for the evaluation of coupling beam characteristics of coupled shear wall", *Asian J. Civil Eng.*, **8**(3), 301-314.

Cai, G.C., Zhao, J., Degée, H. and Vandoren, B. (2016), "Shear capacity of steel fibre reinforced concrete coupling beams using conventional reinforcements", *Eng. Struct.*, **128**, 428-440. https://doi.org/10.1016/j.engstruct.2016.09.056.

Canbolat, B.A., Parra-Montesinos, G.J. and Wight, J.K. (2005), "Experimental study on seismic behavior of high-performance fiber-reinforced cement composite coupling beams", *ACI Struct. J.*, **102**(1), 159-166.

Chaailal, O., Thibodeau, S., Lescelleur, J. and Maleenfant, P. (1996), "Steel fiber or conventional reinforcement for concrete shear walls?", *Concrete International*, **18**(6), 39-42.

CSA Committee A23.3 (2004), Design of concrete structures, Canadian Standard Association; Mississauga, Canada.

Deng, M., Ma, F., Ye, W. and Liang, X. (2018), "Investigation of the shear strength of HDC deep beams based on a modified direct strut-and-tie model", *Constr. Build. Mater.*, **172**, 340-348. https://doi.org/10.1016/j.conbuildmat.2018.03.274.

Gao, D.Y., Shi, K. and Zhao, S.B. (2014), "Calculation method for shear capacity of steel fiber reinforced concrete beam-column joints based on softened strut-and-tie model", *China Civil Eng. J.*, **47**(9), 101-109. https://doi.org/10.15951/j.tmgcxb.2016.02.005.

Hanoon, A.N., Jaafar, M.S., Hejazi, F. and Aziz, F.N.A. (2017), "Strut-and-tie model for externally bonded CFRP-strengthened reinforced concrete deep beams based on particle swarm optimization algorithm: CFRP debonding and rupture", *Constr. Build Mater.*, **147**, 428-447. https://doi.org/10.1016/j.conbuildmat.2017.04.094.

Hwang, S.J. and Lee, H.J. (2002), "Strength prediction for discontinuity regions by softened strut-and-tie model", *J. Struct. Eng.*, **128**(12), 1519-1526. https://doi.org/10.1061/(ASCE)0733-9445(2002)128:12(1519).

Hwang, S.J., Lu, W.Y. and Lee, H.J. (2000), "Shear strength prediction for deep beams", *ACI Struct. J.*, **97**(3), 367-376.

Jia, B. (2012), "Experimental study on steel fiber reinforced concrete coupling beams with different concrete strength", M.Sc. Dissertation, Zhengzhou University, Zhengzhou.

Kuang, J.S. and Baczkowski, B.J. (2006). "Shear capacity of steel fibre reinforced concrete coupling beams", *Joint International Conference on Computing and Decision Making in Civil and Building Engineering*, Montréal, Canada, June.

Kuang, J.S. and Bączkowski, B.J. (2009), "Steel-fibre-reinforced concrete coupling beams subjected to monotonic loading", *Magazine Concrete Res.*, **61**(1), 35-41. https://doi.org/10.1680/macr.2008.00019.

Kuo, W.W., Cheng, T.J. and Hwang, S.J. (2010), "Force transfer mechanism and shear strength of reinforced concrete beams", *Eng. Struct.*, **32**(6), 1537-1546. https://doi.org/10.1016/j.engstruct.2010.02.002.

Kwan, A.K.H. and Zhao, Z.Z. (2002), "Cyclic behaviour of deep reinforced concrete coupling beams", *Proc ICE Structures & Building*, **152**(3), 283-293. https://doi.org/10.1680/stbu.2002.152.3.283.

Lee, H.J., Kuchma, D.A., Baker, W. and Novak, L. (2008), "Design and analysis of heavily loaded reinforced concrete link beams for Burj Dubai", *ACI Struct. J.*, **105**(4), 451-459.

Lequesne, R.D., Parra-Montesinos, G.J. and Wight, J.K. (2013), "Behavior and design of high-performance fiber-reinforced concrete coupling beams and coupled-wall systems", *J. Struct. Eng.*, **139**(8), 1362-1370. https://doi.org/10.1061/(ASCE)ST.1943-541X.0000687.

Li, B. (2012), "Experimental study on steel fiber reinforced concrete coupling beams with different span-depth ratio", M.Sc. Dissertation, Zhengzhou University, Zhengzhou.

Ma X. (2011), "Experimental study on steel fiber reinforced concrete coupling beams with different volume fraction of steel fibers", M.Sc. Dissertation, Zhengzhou University, Zhengzhou.

Matamoros, A.B., Wong, K.H. (2003), "Design of simply supported deep beams using strut-and-tie models", *ACI Struct. J.*, **100**(6), 704-712.

Mihaylov, B.I. and Franssen, R. (2017), "Shear-flexure interaction in the critical sections of short coupling beams", *Eng. Struct.*, **152**, 370-380. https://doi.org/10.1016/j.engstruct.2017.09.024.

Naaman, A.E. (1991), "Bond-slip mechanisms of steel fibers in concrete", *ACI Mater. J.*, **88**(2), 135-145.

Ng, T., Htut, T. and Foster, S.J. (2012), "Fracture of steel fibre reinforced concrete-the unified variable engagement model", M.Sc. Dissertation, The University of New South Wales, Sydney.

NZS 3101 (2006), Concrete structures standard, Part 1 - the design of concrete structures, Standards Association of New Zealand; Wellington, New Zealand.

Parra-Montesinos, G.J. (2005), "High-performance fiber-reinforced cement composites: an alternative for seismic design of structures", *ACI Struct. J.*, **102**(5), 668-675.

Pauletta, M., Luca, D.D. and Russo, G. (2015), "Exterior beam column joints -Shear strength model and design formula", *Eng. Struct.*, **94**, 70-81. https://doi.org/10.1016/j.engstruct.2015.03.040.

Romualdi, J.P. and Mandel, J.A. (1964), "Tensile strength of concrete affected by uniformly distributed and closely spaced short lengths of wire reinforcement", *ACI Mater. J.*, **61**(6), 657-672.

Schlaich, J., Schäfer, K. and Jennewein, M. (1987), "Toward a consistent design of structural concrete", *PCI J.*, **32**(3), 74-150.

Thomas, T.C.H, Mo, Y.L. (2010), *Unified Theory of Concrete Structures*, Wiley Press, Chichester, United Kingdom.

Yavuz, G. (2016), "Shear strength estimation of RC deep beams using the ANN and strut-and-tie approaches", *Struct. Eng. Mech.*, **57**(4), 657-680. https://doi.org/10.12989/sem.2016.57.4.657.

Zhang, H.Z., Zhang, R.J. and Huang, C.K. (2007), "Experimental study of shear resistance of steel fiber reinforced high strength concrete coupling beams". *China Civ. Eng. J.*, **40**(11), 15-22. https://doi.org/10.15951/j.tmgcxb.2007.11.005

CC

Appendix

a_s	depth of the main inclined strut
$A_{sf,v}$	equivalent cross section area of the vertical tie of steel fibers
A_{str}	effective area of main inclined strut
A_{sv}	cross sectional area of stirrups vertical tie
A_{sv1}	cross section area of single stirrup
b	width of coupling beam section
b_s	width of the main inclined strut
d	effective height of coupling beam
d'	distance from centroid of the compression reinforcement to compression zone's edge
D_{sf}	type impact coefficient of steel fiber
E_s	elastic modulus ratio of longitudinal reinforcement
E_c	elastic modulus ratio of concrete
f_{ce}	effective compressive strength of strut
f_{ct}	mean tensile strength of concrete matrix
f_{fc}'	cylinder compressive strength of fiber concrete
f_{fct}	steel fiber concrete tensile strength
f_{fcu}	cube compressive strength of fiber concrete
f_{sf}	average shear stress of steel fibers
f_y	tensile strength of longitudinal bar
f_{yf}	ultimate tensile strength of steel fiber
f_{yv}	yielding stress of stirrups
F_c	bearing capacity of main inclined strut
F_{sf}	bearing capacity of steel fibers vertical tie
F_{sv}	bearing capacity of stirrups vertical tie
F_v	bearing capacity of vertical tie
h	height of coupling beam section
jd	distance of the lever arm from the resultant compressive force to the centroid of the longitudinal tension reinforcement
kd	depth of compression zone at cross section
k_b	correlation coefficient of steel fiber type
l_j	projected length of the main crack in the horizontal direction
l_n	length of coupling beam
l_n/h	span-to-depth ratio
n	elastic modulus ratio of longitudinal reinforcement to concrete
n_{sv}	number of stirrups
V_c	calculated shear strength
V_{sf}	volume fraction of steel fiber
V_t	measured shear strength
α_f	length to diameter ratio of steel fiber
θ_c	the angle between the main crack and the horizontal direction
θ_f	inclination angle of main inclined strut
$\sigma_{d,\max}$	maximum compressive stress
$\tau_{sf,\max}$	maximum bond shear stress between steel fiber and concrete
ρ	reinforcement ratio of longitudinal bar
ρ'	compression reinforcement ratio
ρ_v	reinforcement ratio of stirrups
η_1	coefficient of shear resistance
η_2	direction coefficient of steel fiber
ζ	softening coefficient of concrete